Research Article

Prony Analysis for Power System Transient Harmonics

Li Qi, Lewei Qian, Stephen Woodruff, and David Cartes

The Center for Advanced Power Systems, Florida State University, Tallahassee, FL 32310, USA

Proliferation of nonlinear loads in power systems has increased harmonic pollution and deteriorated power quality. Not required to have prior knowledge of existing harmonics, Prony analysis detects frequencies, magnitudes, phases, and especially damping factors of exponential decaying or growing transient harmonics. In this paper, Prony analysis is implemented to supervise power system transient harmonics, or time-varying harmonics. Further, to improve power quality when transient harmonics appear, the dominant harmonics identified from Prony analysis are used as the harmonic reference for harmonic selective active filters. Simulation results of two test systems during transformer energizing and induction motor starting confirm the effectiveness of the Prony analysis in supervising and canceling power system transient harmonics.

1. INTRODUCTION

In today's power systems, the proliferation of nonlinear loads has increased harmonic pollution. Harmonics cause many problems in connected power systems, such as reactive power burden and low system efficiency. Harmonic supervision is highly valuable in relieving these problems in power transmission systems. Further, shunt active filters can be connected in power distribution systems to improve power quality. With the compensating currents injected by the active filters, the currents are cleaner and less harmonic pollution induced by the nonlinear load affects the operation of the connected power grid.

Normally, Fourier transform-based approaches are used for supervising power system harmonics. In order to maintain the computational accuracy of Fourier transform, the stationary and periodic characteristics of signals are generally required. However, power system loads, especially industrial loads, are often dynamic in nature, and produce time varying currents. In this paper, harmonics with time varying magnitudes in power systems are called power system transient harmonics. The accuracy of Fourier transform is affected when these transient or time varying harmonics exist. To achieve controllable harmonic cancellation for power quality improvement, low filter ratings, and bandwidth requirement reductions, harmonic selective active filters are used in power distribution systems. Accurate harmonic reference generation of the harmonics is the key to these harmonic selective active filters. Some of the harmonic reference generation methods require PLL (phase locked loops) or frequency estimators for identifying the specific harmonic frequency before the corresponding reference is generated [1–4].

In this paper, Prony analysis is applied as an analysis method for harmonic supervisors and as a harmonic reference generation method for harmonic selective active filters. Prony analysis, as an autoregressive spectrum analysis method, has some valuable features. Prony analysis does not require frequency information prior to filtering. Additional PLL or frequency estimators described earlier in existing active filters are no longer necessary. Prony-analysis-based harmonic supervisors and active filters are thus applicable in situations where there is no prior knowledge of the frequencies. Due to the ability to identify the damping factors of transients, Prony analysis can accurately identify growing or decaying components of signals. Transient harmonics thus can be correctly identified from Prony analysis for the Prony-based harmonic supervision and the harmonic reference generation.

Some results in Prony analysis for supervising and canceling power system transient harmonics are presented in this paper. Two important operations in power transmission and distribution systems, energizing a transformer and starting of an induction motor, induce transient harmonics and have adverse effects on power system quality [5–7]. With an appropriate Prony algorithm selected, nonstationary or time

varying transient harmonics during transformer energizing and motor starting are identified. The harmonic results from Prony analysis and Fourier transform are compared. The effectiveness of the Prony-based harmonic selective active filter is verified by simulation results. The advantages and disadvantages of the application of Prony analysis in harmonic supervisors and active filters are also discussed.

In Section 2 of this paper, Prony analysis, including theory basis, selection of Prony algorithm, tuning Prony parameters, and comparison of Prony analysis and Fourier Transform, is described. In Section 3, two test systems, which respectively represent a part of a transmission system and a distribution system, to study power system transient harmonics are described. In Section 4, case studies using Prony-based harmonic supervisors and harmonic selective active filters are presented. In Section 5, some conclusions are drawn.

2. PRONY ANALYSIS

Since Prony analysis was first introduced into power system applications in 1990, it has been widely used for power system transient studies [8, 9], but rarely used for power quality studies. In this section, the basis for Prony analysis is presented. Then, the selection of an appropriate Prony algorithm from three existing algorithms is discussed. A general guidance of tuning Prony analysis parameters is given. At last, Prony and Fourier analyses are compared.

2.1. Basis of Prony analysis

Prony analysis is a method of fitting a linear combination of exponential terms to a signal as shown in (1) [10]. Each term in (1) has four elements: the magnitude A_n, the damping factor σ_n, the frequency f_n, and the phase angle θ_n. Each exponential component with a different frequency is viewed as a unique mode of the original signal $y(t)$. The four elements of each mode can be identified from the state space representation of an equally sampled data record. The time interval between each sample is T:

$$y(t) = \sum_{n=1}^{N} A_n e^{\sigma_n t} \cos\left(2\pi f_n t + \theta_n\right), \quad n = 1, 2, 3, \ldots, N. \quad (1)$$

Using Euler's theorem and letting $t = MT$, the samples of $y(t)$ are rewritten as (2)

$$y_M = \sum_{n=1}^{N} B_n \lambda_n^M, \quad (2)$$

$$B_n = \frac{A_n}{2} e^{j\theta_n}, \quad (3)$$

$$\lambda_n = e^{(\sigma_n + j2\pi f_n)T}. \quad (4)$$

Prony analysis consists of three steps. In the first step, the coefficients of a linear predication model are calculated. The linear predication model (LPM) of order N, shown in (5), is built to fit the equally sampled data record $y(t)$ with length M. Normally, the length M should be at least three times

larger than the order N:

$$y_M = a_1 y_{M-1} + a_2 y_{M-2} + \cdots + a_N y_{M-N}. \quad (5)$$

Estimation of the LPM coefficients a_n is crucial for the derivation of the frequency, damping, magnitude, and phase angle of a signal. To estimate these coefficients accurately, many algorithms can be used. A matrix representation of the signal at various sample times can be formed by sequentially writing the linear prediction of y_M repetitively. By inverting the matrix representation, the linear coefficients a_n can be derived from (6). An algorithm, which uses singular value decomposition for the matrix inversion to derive the LPM coefficients, is called SVD algorithm,

$$\begin{bmatrix} y_N \\ y_{N+1} \\ \vdots \\ y_{M-1} \end{bmatrix} = \begin{bmatrix} y_{N-1} & y_{N-2} & \cdots & y_0 \\ y_N & y_{N-1} & \cdots & y_1 \\ \vdots & \vdots & \vdots & \vdots \\ y_{M-2} & y_{M-3} & \cdots & y_{M-N-1} \end{bmatrix} \begin{bmatrix} a_1 \\ a_2 \\ \vdots \\ a_N \end{bmatrix}. \quad (6)$$

In the second step, the roots λ_n of the characteristic polynomial shown as (7) associated with the LPM from the first step are derived. The damping factor σ_n and frequency f_n are calculated from the root λ_n according to (4):

$$\lambda^N - a_1 \lambda^{N-1} - \cdots - a_{N-1}\lambda - a_N \\ = (\lambda - \lambda_1)(\lambda - \lambda_2) \cdots (\lambda - \lambda_n) \cdots (\lambda - \lambda_N). \quad (7)$$

In the last step, the magnitudes and the phase angles of the signal are solved in the least square sense. According to (2), (8) is built using the solved roots λ_n:

$$\mathbf{Y} = \boldsymbol{\phi}\mathbf{B}, \quad (8)$$

$$\mathbf{Y} = \begin{bmatrix} y_0 & y_1 & \cdots & y_{M-1} \end{bmatrix}^T, \quad (9)$$

$$\boldsymbol{\phi} = \begin{bmatrix} 1 & 1 & \cdots & 1 \\ \lambda_1 & \lambda_2 & \cdots & \lambda_N \\ \vdots & \vdots & \vdots & \vdots \\ \lambda_1^{M-1} & \lambda_2^{M-1} & \cdots & \lambda_N^{M-1} \end{bmatrix}, \quad (10)$$

$$\mathbf{B} = \begin{bmatrix} B_1 & B_2 & \cdots & B_N \end{bmatrix}^T. \quad (11)$$

The magnitude A_n and phase angle θ_n are thus calculated from the variables B_n according to (3).

The greatest advantage of Prony analysis is its ability to identify the damping factor of each mode in the signal. Due to this advantage, transient harmonics can be identified accurately.

2.2. Selection of Prony analysis algorithm

Three normally used algorithms to derive the LPM coefficients, the Burg algorithm, the Marple algorithm, and the SVD (singular value decomposition) algorithm [11–13], are compared for implementing Prony analysis in transient harmonic studies. Basically, the three algorithms use different objective functions to estimate LPM coefficients. In our

Table 1: Estimated dominant harmonics (EDH) on a nonstationary signal.

	EDH	Ideal	Burg	Marple	SVD
	#1	60	60.1690	59.9986	59.9987
	#2	300	298.2309	279.3917	299.9951
Frequencies (Hz)	#3	420	419.3031	420.0081	420.0138
	#4	660	657.8118	659.9380	659.9578
	#5	780	779.1504	779.9914	780.0137
	#1	0	−0.0037	−0.0027	−0.0012
	#2	−6	−1.3173	0.2127	−6.0403
Damping factors (s^{-1})	#3	−4	−0.0940	0.1245	−4.0638
	#4	0	−0.5625	−0.1881	−0.1097
	#5	0	−3.4003	−0.6494	−0.1752
	#1	1	1.0001	0.9997	1.0002
	#2	0.2	0.1478	0.1441	0.2002
Magnitudes (A)	#3	0.1	0.0819	0.0809	0.1003
	#4	0.02	0.0184	0.0203	0.0204
	#5	0.01	0.0104	0.0107	0.0103
	#1	0	3.1693	0.0320	3.1693
	#2	45	79.0299	44.9906	45.0567
Phase angles (degree)	#3	30	41.4376	30.2150	29.9158
	#4	0	36.8397	−0.8574	0.7913
	#5	0	12.7567	0.1850	0.3631

study, the recursive Burg and Marple algorithms were programmed in Matlab according to the description by Kay and Marple [13], while the nonrecursive SVD algorithm utilized the Matlab pseudoinverse function *pinv*. This *pinv* function uses LAPACK routines to compute the singular value decomposition for the matrix inversion [14].

To choose the appropriate algorithm, the three algorithms are applied on the same signals with the same Prony analysis parameters. The signals are synthesized in the form of (1) plus a noise to approximate real transient signals. The synthesized signal includes time varying harmonics. No sudden change occurs in the signal. The eventual variation of these harmonics with time can be described or modeled with exponential functions. The noise level is much smaller compared to the least harmonic component in the synthesized signal, which can be achieved by appropriately preprocessing technique. The sampling frequency is selected equal to four times of the highest harmonic and the length of data is six times of one cycle of the lowest harmonic [15]. The algorithm with the best overall performance on identifying frequency, damping factor, magnitude, and phase angle is selected as the appropriate algorithm.

Table 1 lists the estimation results from the three algorithms on one transient signal. More estimation results on synthesized power system signals were derived by the authors for different studies [16]. The dominant harmonics, including the fundamental (60 Hz), the fifth, seventh, eleventh, and thirteenth harmonics, are identified. From the table, the damping factors from the SVD algorithm are much closer to the ideal damping factors than those from the Marple and the Burg algorithms. Additionally, the frequency, magnitude,

and phase angles from the SVD algorithm are more precise. From comparison on the estimation results of various signals to approximate power system transient harmonics, the SVD algorithm has the best overall performance on all estimation results and thus is selected as the appropriate algorithm for our study.

2.3. Tuning of Prony analysis parameters

Since the estimation of data is an ill-conditioned problem [12, 13], one algorithm could perform completely differently on different signals. Therefore, Prony analysis parameters should be adjusted by trial and error to achieve most accurate results at different situations. Although the parameter tuning is a trial and error process, there are still some rules to follow. A general guidance on parameter adjustment is given in the rest of this section.

A technique of shifting time windows by Hauer et al. [8] is adopted for continuously detecting dominant harmonics in a Prony-analysis-based harmonic supervisor. The shifting time window for Prony analysis has to be filled with sampled data before correct estimation results are derived. The selection of the equal sampling intervals between samples and the data length in an analysis window depends on the simulation time step and the estimated frequency range. The equal sampling frequency follows Nyquist sampling theorem and should be at least two times of the highest frequency in a signal. Since the Prony analysis results are not accurate for too high sampling frequency [15], two or three times of the highest frequency is considered to produce accurate Prony analysis results and was used in our study. Similarly, the length of Prony analysis window should not be too long or too short [15]. The length of the Prony analysis window should be at least one and half times of one cycle of the lowest frequency of a signal.

Besides the sampling frequency and the length of Prony analysis window, the LPM order is another important Prony analysis parameter. A common principle is that the LPM order should be no more than one thirds of the data length [8, 15]. The data length and LPM order could be increased together in order to accommodate more modes in simulated signals. It is quite difficult to make the first selection of the LPM order since the exact number of modes of a real system is hard to determine. In our study, a guess of 14 is a good start. If the order is found not high enough, the data length of the Prony analysis window should be increased in order to increase the LPM order.

The general guidance for tuning Prony analysis parameters is applicable to other applications of Prony analysis. Not requiring specific frequency of a signal for Prony analysis, the tuning method is not sensitive to fine details of the signal and thus extensive retuning for different types of transients in the same system is unlikely to be necessary for Prony analysis.

2.4. Prony analysis and Fourier transform

As described earlier, Prony analysis can accurately analyze exponential signals. In power systems, the Fourier transform is

widely used for spectrum analysis. However, signals must be stationary and periodic for the finite Fourier transform to be valid.

The following analysis explains why results from the Fourier transform are inaccurate for exponential signals. The general form of a nonstationary signal can be found in (1). If the phase angle of the signal is equal to zero, and the magnitude is equal to unity, then the general form can be simplified into the signal shown in (12). The initial time of the Fourier analysis is taken to be t_0 and the duration of the Fourier analysis window is T, which is equal to the period of the analysis signal for accurate spectrum analysis:

$$x(t) = e^{\sigma t} \cos(2\pi f t). \tag{12}$$

The Fourier transform during t_0 to $t_0 + T$ is calculated as (13). The first term on the right-hand side of (13) is equal to zero according to (14). Therefore, the magnitude of the signal in terms of the Fourier transform is given in (15). The ratio k between the magnitude of the Fourier transform in (15) and the actual magnitude $e^{\delta t_0}$ is shown as (16), which indicates the average effect of the Fourier analysis window:

$$
\begin{aligned}
a_n &= \frac{2A}{T} \int_{t_0}^{t_0+T} e^{\delta t} \cos(2\pi f t) \cos(2\pi f t) dt \\
&= \frac{A}{T} \int_{t_0}^{t_0+T} e^{\delta t} \left[\cos(4\pi f t) + 1 \right] dt \\
&= \frac{A}{T} \int_{t_0}^{t_0+T} e^{\delta t} \cos(4\pi f t) dt + \frac{A}{T} \int_{t_0}^{t_0+T} e^{\delta t} dt,
\end{aligned}
\tag{13}
$$

$$
\begin{aligned}
&\frac{1}{T} \int_{t_0}^{t_0+T} e^{\delta t} \cos(4\pi f t) dt \\
&= \frac{1}{T} \frac{e^{\delta t}}{\delta^2 + (4\pi/T)^2} \left[-\delta \cos(4\pi f t) \right. \\
&\qquad\qquad \left. + 4\pi f \sin(4\pi f t) \right] \Big|_{t_0}^{t_0+T} = 0,
\end{aligned}
\tag{14}
$$

$$
\begin{aligned}
a_n &= \frac{1}{T} \int_{t_0}^{t_0+T} e^{\delta t} dt = \frac{1}{\delta T} e^{\delta t} \Big|_{t_0}^{t_0+T} \\
&= \frac{1}{\delta T} \left[e^{\delta(t_0+T)} - e^{\delta(t_0)} \right] = e^{\delta t_0} \frac{(e^{\delta T} - 1)}{\delta T},
\end{aligned}
\tag{15}
$$

$$k = \frac{e^{\delta T} - 1}{\delta T}. \tag{16}$$

Let us consider a fast damping signal and a slow damping signal with damping factors δ equal to -100 and -0.01, respectively. If the frequency f is equal to 60 Hz, then the duration T is equal to 0.0167 seconds. According to (16), the ratio k between the Fourier magnitude and the real magnitude is derived as 0.4861 and 0.9999. If the damping factor is equal to zero or the signal is nonexponential, the ration k becomes one and the Fourier magnitude exactly reflects the real signal magnitude. Therefore, with rapid decaying factors, the magnitude derived from Fourier transform is not even close to its actual magnitude. If the analysis window is longer, the signal magnitude from Fourier is even less accurate. For example, if the time duration T of the analysis window is two cycles long and the damping ratio is -100, then the ratio between the Fourier magnitude and the actual magnitude decreases to 0.2888. Therefore, with rapidly decaying signals,

Fourier analysis results depend greatly on the length of the analysis window. Prior knowledge of the specific frequency involved is quite important for selecting the proper length of the Fourier analysis window and getting accurate results.

A conflict exists in selecting the length of the Fourier analysis window. In order to reduce the error due to the average effect of the analysis window, the length of the Fourier analysis window should decrease. However, the fewer periods there are in the record, the less random noise gets averaged out and the less accurate the result will be. Some compromise must be made between reducing noise effects and increasing Fourier analysis accuracy. The length of the Prony analysis window is not as sensitive as the Fourier analysis window. If the frequency of an analyzed signal is within a certain range, it is not necessary to change the length of the analysis window. A long window can be used to deal with noise and still detect decaying modes accurately.

3. TEST SYSTEMS

Two test systems are used to verify the effectiveness of Prony analysis on transient harmonic supervision and harmonic cancellation. The parameters of the test systems can be found in Tables A.1–A.10 in the appendix.

Test system 1 models a part of a transmission system at the voltage level of 500 kV and is used to simulate transformer energization. Test system 2 models a part of a distribution system at the voltage level of 480 V and is used to simulate motor starting. The test systems are realized in the simulation environment of PSIM and Matlab.

3.1. Test system 1

Figure 1 shows the configuration of test system 1, which includes a voltage source, a local LC load bank, three-phase transformer, and a harmonic supervisor. The system is designed to be resonant at forth harmonic [17].

In order to simulate inrush currents during transformer energization, the transformer has a saturable magnetizing branch, whose saturation characteristic is described in the appendix. Since large transformers in transmission systems are normally energized before connected to any load, the secondary side of the simulated transformer is at no load condition. The voltages and currents at the transformer primary side are inputs of the harmonic supervisor; while the outputs are the harmonic description of the voltages and currents. According to the harmonic analysis method, the description can be harmonic magnitudes and phase angles from Fourier analysis or harmonic waveforms from Prony analysis.

In our study, the Fourier transform analysis utilizes the function FFT provided in the SimPowerSystems Toolbox in Matlab. This FFT function adopts a fast Fourier transform algorithm usually used in power systems. One cycle of simulation has to be completed before the outputs give the correct magnitude and angle since the FFT function uses a running average window [17]. As described earlier, shifting time windows is used in Prony analysis for continuously detecting dominant harmonics. In this Prony-based harmonic
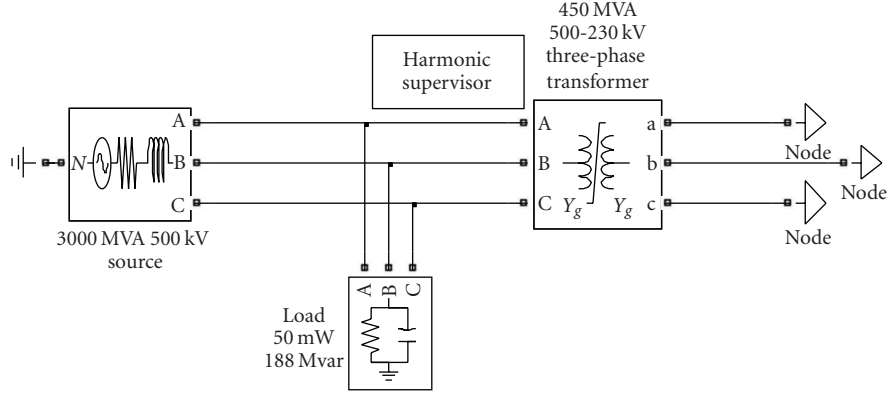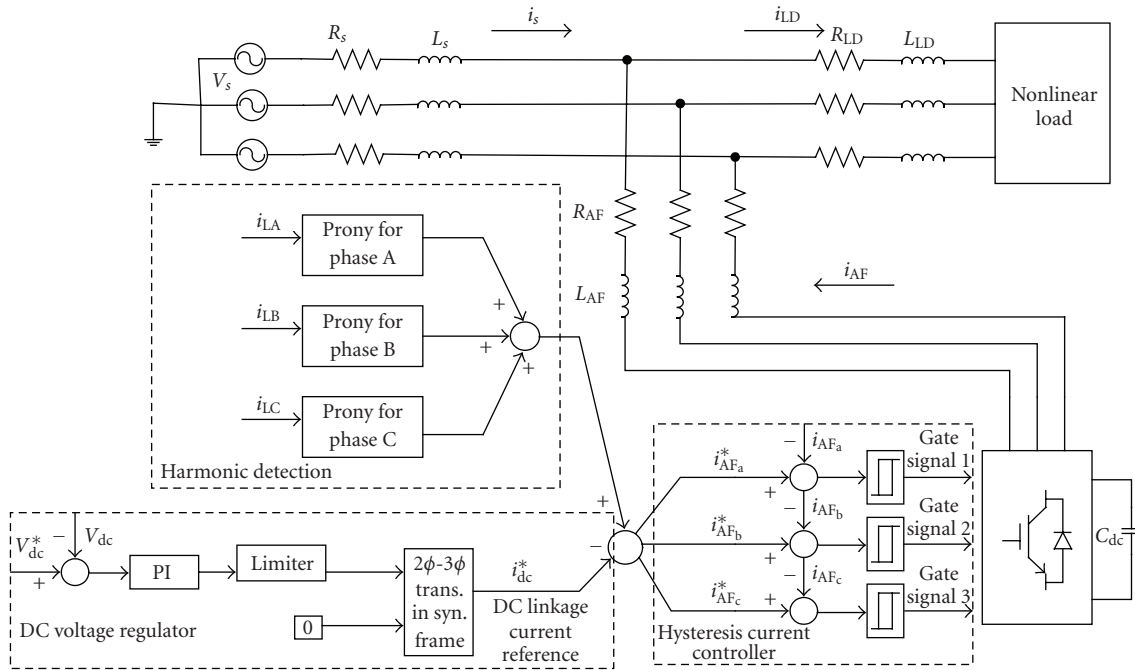
FIGURE 1: Configuration of test system 1.

FIGURE 2: Configuration of test system 2.

supervisor for transformer energizing, since the fundamental frequency is considered as the lowest frequency, the time duration of Prony analysis window is 0.036 second, which is longer than two cycles of the fundamental frequency. The time interval between any two windows is 0.6 millisecond. The sampling frequency is 833 Hz, which is sufficient enough for identifying up to 13th harmonic in the system. The data length within a time window is 60. The order of linear prediction model is 20, which is equal to one third of the data length. If the length of the analysis window is shorter than two cycles of the analyzed frequency, the Prony analysis results would be inaccurate. On the other hand, if the analysis window is longer, the accuracy of the analysis results would not change, but unnecessary burden is added on the computation of Prony analysis.

3.2. Test system 2

Figure 2 shows the configuration of test system 2, which includes a voltage source, a nonlinear load including an induction motor and a diode rectifier load, a harmonic selective active filter using a three-phase active voltage source IGBT (insulated gate bipolar transistor) converter, and controller systems associated with the active filter. The nonlinear load represents a type of load combination, induction motors plus power electronic loads, in power distribution systems.

The induction motor is modeled by a set of nonlinear equations [18], which are different from the commonly used linear equivalent circuit to model induction motors in power quality studies [5]. The two modeling methods are equally efficient for detecting steady state harmonics. The nonlinearity

consists of the stator and rotor currents to obtain electrical torque and rotor position to derive voltages. These nonlinearities are particularly important during motor starting for motor currents and rotor speed rise in amplitude from zero to their steady-state values. Therefore, the usage of the nonlinear detailed model allows the detailed description of motor starting transients.

The control system of the active filter can be separated into two parts, one for controlling harmonic reference generation using Prony analysis or Fourier transform and one for controlling the DC link bus voltage. The dominant harmonics of the three-phase load currents are derived from Prony analysis or Fourier transform and used as the reference for the harmonic selective active filter. To control DC bus voltage, a PI (proportional integral) controller is used to generate the DC link current reference. Three hysteresis controllers then generate gate signals for the IGBT converter.

The function FFT mentioned in test system 1 is also used in test system 2 for the Fourier-based active filter. The technique of shifting time windows is adopted in the Prony-based harmonic selective active filter as well. As described earlier, some Prony analysis parameters used earlier in transformer energizing are adjusted by trial and error to achieve most accurate results in motor starting. In this Prony-based active filter to cancel transient harmonics during motor starting, since there could be subharmonics during motor starting, the time duration of the Prony analysis window is 0.024 second. The sampling frequency is 2500 Hz, which is sufficient to identify up to the 20th harmonic in the system. With the careful selection of these Prony analysis parameters, the spurious harmonics besides the dominant harmonics are small enough that their effects can be neglected.

4. CASE STUDIES

Using the SVD algorithm discussed in Section 2, two cases were studied to implement Prony analysis for power quality study. The first case studies the harmonic supervision of the test transmission system 1 shown in Figure 1. The harmonic description from the Prony-analysis- and Fourier-transform-based harmonic supervisors is compared. The second case studies the harmonic cancellation of the test distribution system 2 shown in Figure 2. The results from the Prony-based harmonic selective active filter are compared with the results from the Fourier-based active filter. The power quality improvement by the Prony-based harmonic selective active filter is verified.

4.1. Case 1: harmonic supervision during transformer energizing

Transformers exhibit high inrush currents upon initial energization in order to energize the transformer core. These high transformer inrush currents are full of harmonics. These harmonics deteriorate power quality and may cause problems in operation, such as overvoltage by exciting system resonance [5]. In the simulated system, the forth harmonic caused by transformer energizing induces resonance in the system.

Both even and odd harmonic components are produced during the transformer energizing. Among them, the second harmonic is dominant harmonic. The magnitudes of the harmonics during energizing vary with time [5]. No abrupt changes are found in time varying harmonic magnitudes. An exponential function thus is able to approximate these time varying harmonics.

As described earlier, the Fourier transform is normally used to supervise power system harmonics in power systems. To demonstrate the effectiveness of the Prony analysis for harmonic supervision, the outputs from the Fourier-transform-based harmonic supervisor are compared with those from the Prony-analysis-based harmonic supervisor. Figure 3 shows the harmonic supervision results of test system 1 using the Prony-analysis- and Fourier-transform-based harmonic supervisors. To simulate transformer energization, the remnant fluxes of 0.8, −0.4, and 0.4 p.u. are specified, respectively, for phases A, B, and C of the three-phase transformer. The transformer is energized at the beginning of the simulation. At the same time the harmonic supervisors take action.

Figures 3(a) and 3(b) show the fundamental and fourth harmonic voltage waveforms derived from Prony and the magnitudes from FFT. During the time period shown in the figures, the fundamental component is almost kept constant and the 4th harmonic of voltage decays fast. For the fundamental component, the magnitude obtained from FFT agrees with the magnitude of the fundamental voltage waveform from Prony. However, for the fourth harmonic, the magnitude from FFT is much smaller than the magnitude from Prony. This is because the magnitude derived from FFT is the average magnitude of the waveform in the FFT running window.

Figures 3(c) and 3(d) show the fundamental and second harmonic currents from Prony analysis and the magnitudes from FFT. During the time period shown in the figures, the fundamental component decays and the second harmonic current first grows and then decays. The decaying and growing speeds are slow. It is found that the magnitudes of the waveforms from Prony analysis agree well with the magnitudes from FFT. The periodic change in the second harmonic magnitude as seen from Figure 3(d) indicates that certain low frequency components exist in the second harmonic current from FFT. Therefore, the magnitude of the second harmonic current from FFT is a little higher than that of the second harmonic current waveform from Prony analysis, which is considered to contain only the second harmonic current.

The actual signals and their corresponding variables estimated from Prony are compared in Figure 4. Figures 4(a) and 4(b) show the actual and estimated transformer voltages of phases A and B. The estimated voltages fit well with the actual signal. Figures 4(c) and 4(d) show the actual and estimated transformer current and total load current of phase A. It can be found that, indeed, some nonlinearity, especially at the beginning of transformer energizing is lost by Prony analysis. The total load current is better estimated than the transformer current since some nonlinearity of the transformer is lessened by the linearity of the LC load bank. It is found

(a) Fundamental voltage (phase A).

(b) Fourth harmonic voltage (phase A).

(c) Fundamental current (phase A).
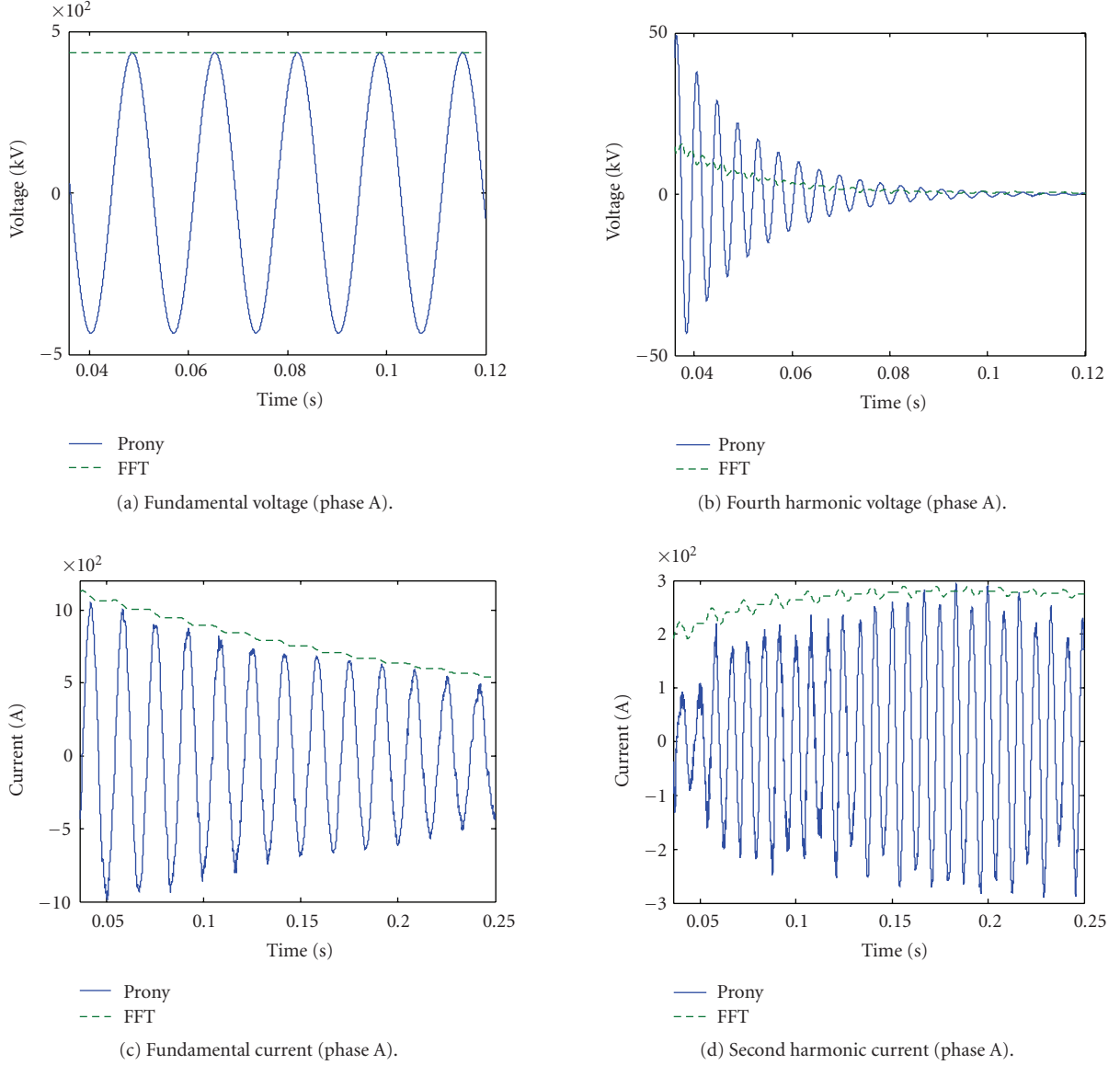
(d) Second harmonic current (phase A).

FIGURE 3: Prony and FFT results of case 1.

that after the large nonlinearity at the initial stage the transformer inrush current and load current can be well estimated with Prony analysis.

The effectiveness of the Prony-based harmonic supervisor is verified from the results shown earlier. From the comparison shown above, without damping or with small damping, the harmonic supervision results from Prony analysis and FFT are almost equal in the sense of harmonic magnitudes. With fast damping, Prony analysis derives more accurate harmonic supervision results than FFT does.

4.2. Case 2: harmonic cancellation during motor starting

During motor starting, the magnitude of the starting current can become as high as several times of the rated cur-

rent. By flowing through system impedances, this large current will cause voltage sags, which dim lights, cause contactors to drop out, and disrupt sensitive equipment [5]. This high motor starting current contains mainly exponentially decaying fundamental current and a small portion of harmonic or subharmonic currents. Due to the exponentially decaying fundamental current, the load voltage changes exponentially. A rectifier load is connected in paralleled with the induction motor and produces load currents full of harmonics. Since the voltage supplied to the rectifier load is exponentially changing during motor starting, the harmonic currents drawn by the rectifier load appear as exponentially changing harmonic currents. Detecting and canceling harmonics in the total load currents during motor starting are critical to overall power system reliability and power quality.

(a) Transformer voltage (phase A).

(b) Transformer voltage (phase B).

(c) Transformer current (phase A).

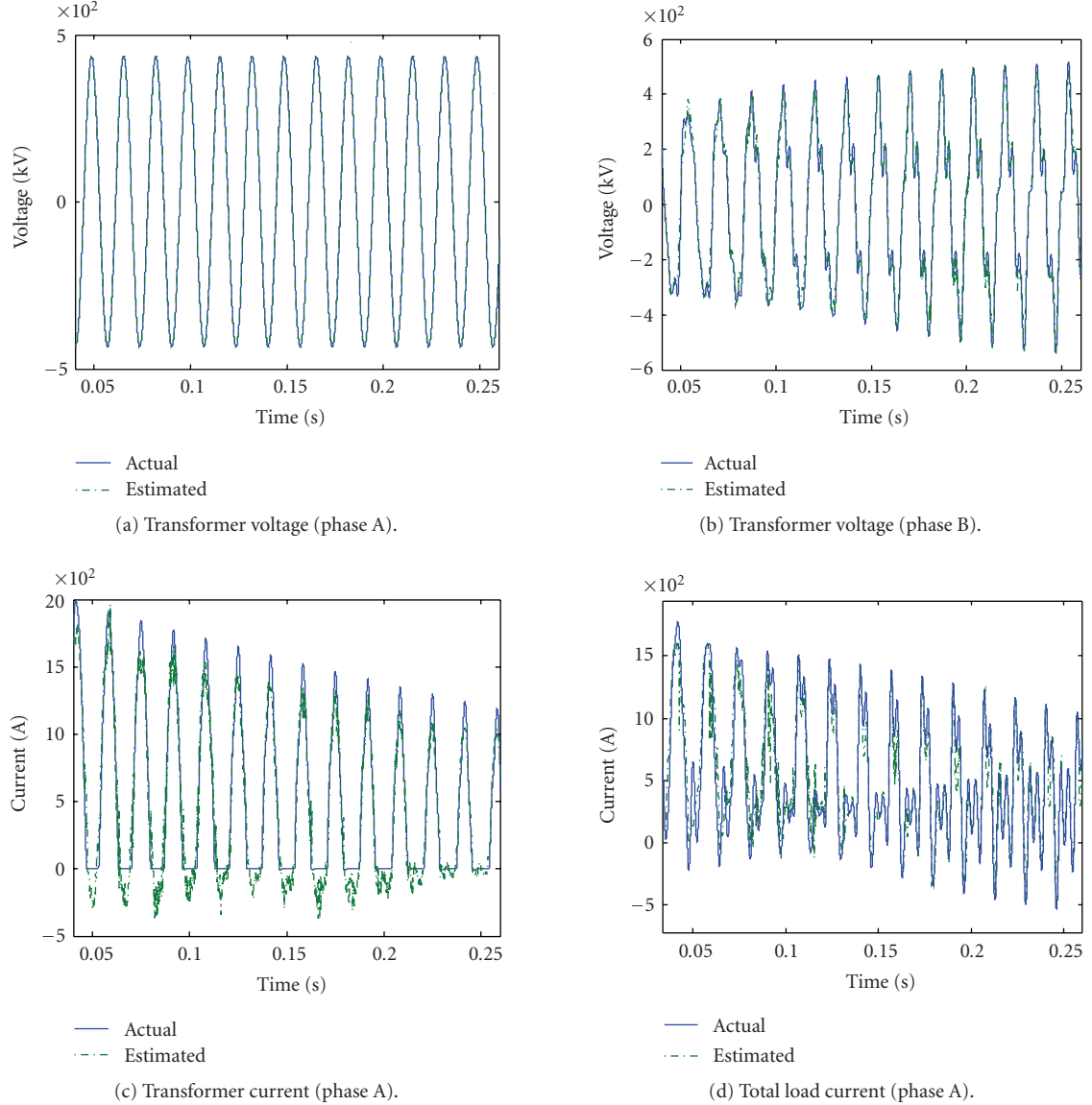(d) Total load current (phase A).

FIGURE 4: Actual and estimated voltages and currents.

With the accuracy of Prony analysis in harmonic supervisors verified, Prony analysis can be used in close loop controllers, such as active filters, to improve power quality. In this case, the Prony-based harmonic selective active filter is used to conduct harmonic cancellation during motor starting transient. This Prony-based active filter has been tested with an ideal harmonic current load before being applied during motor starting [16].

Figure 5 shows the simulation results of the transient harmonic cancellation by the Prony-based active filter during motor starting. The motor starts with free acceleration since its load torque is a small constant torque equal to 0.02 Nm. At first, the system runs at steady state with only ideal diode rectifier load connected. After the active filter takes action at 0.06 second, the induction motor is switched into the test system at 0.12 second. The motor starting transient lasts for sev-

eral cycles and dies down approximately at 0.2 second. The test system finally settles down at steady state with both motor and diode rectifier load connected. At steady state, the ideal diode rectifier load generates stationary harmonic currents, mainly the fifth and seventh harmonic currents in the test system. The stationary harmonic cancellation with the diode rectifier load has been verified by the authors [15].

Table 2 shows the three most dominant frequencies identified from Prony analysis at three selected time instants. The three time instants are selected arbitrarily from the time duration before, during, and after motor starting transient. It is found that the second dominant harmonic current changes from the fifth harmonic current before motor starting to the second harmonic current after motor starting. This change of dominant harmonics is expected since the second harmonic current is induced by starting an induction motor [5]. At the

(a) Source currents.

(b) Load currents (phase A).

(c) Source currents (phase A) during motor starting.

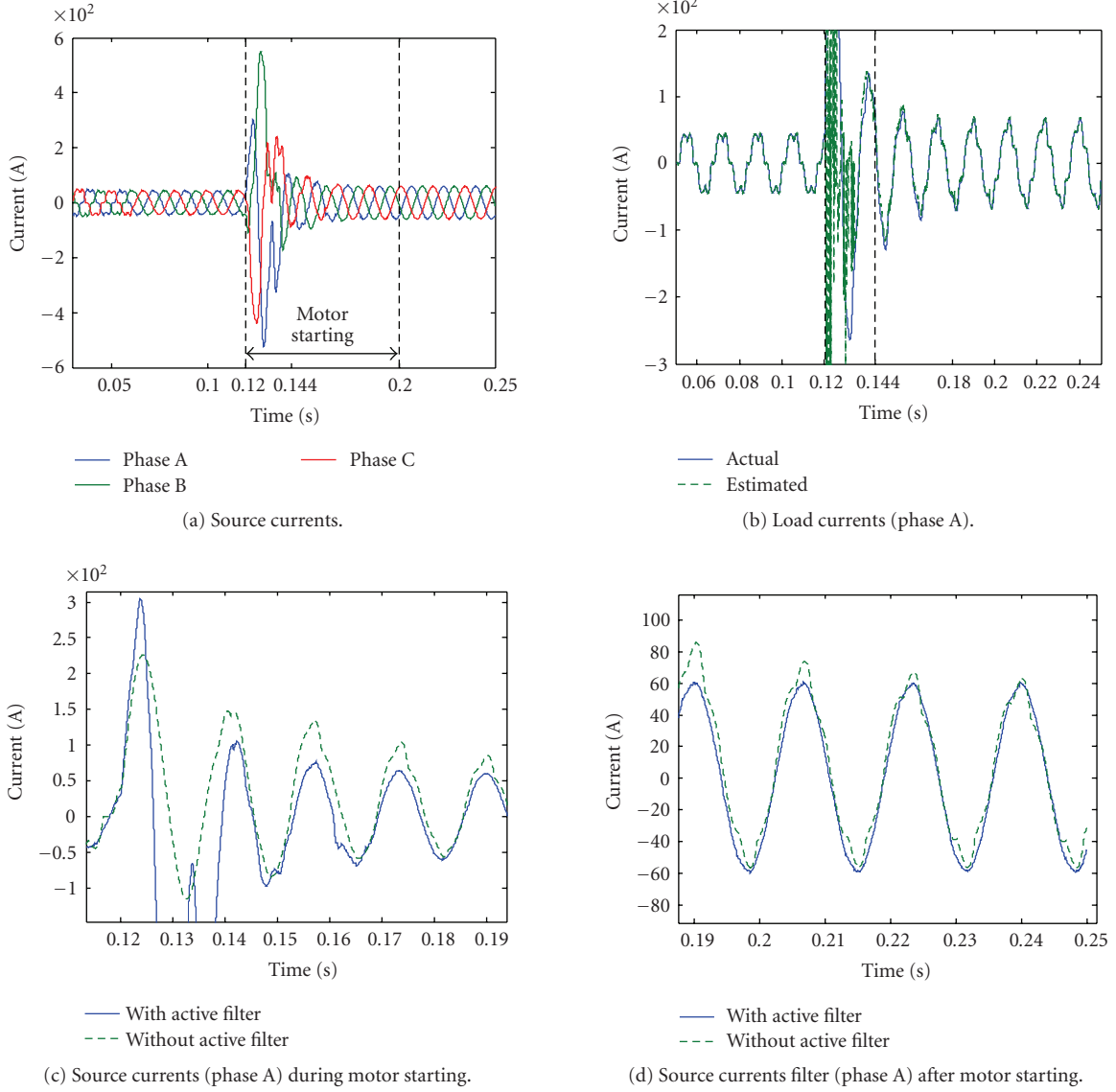(d) Source currents filter (phase A) after motor starting.

FIGURE 5: Simulation results of case 2 (Prony).

beginning of the motor starting, this second harmonic is especially high due to asymmetric waveform of the motor current. This second harmonic current is damped out quickly with a high damping factor. The magnitudes of the fifth and seventh harmonic currents change exponentially since the supplied voltage exponentially changes during motor starting. The magnitudes of the fifth and seventh harmonic currents are almost kept constant before and after motor starting transients. The magnitude of the fundamental current increases after motor starting since the total load current increases with the motor load added as a part of the system load.

Figure 6 shows the simulation results of the transient harmonic cancellation by the Fourier-based active filter during motor starting. The y-axis in each graph of Figure 6 has the same range as the corresponding graph in Figure 5. During

TABLE 2: Estimated dominant harmonics (EDH) of case2.

	EDH	$T = 0.1$	$T = 0.1786$	$T = 0.2403$
Frequencies (Hz)	#1	60.0880	60.9739	60.0395
	#2	300.2141	121.2281	299.8692
	#3	420.4627	299.9159	420.9291
Magnitudes (A)	#1	44.0179	82.5488	58.9011
	#2	8.8723	12.0627	9.2252
	#3	3.0207	8.8103	3.4445
Damping factors (s^{-1})	#1	0.0450	−14.6057	0.1782
	#2	0.2094	−116.4742	−0.1920
	#3	0.4268	−2.8884	−0.5291

the stationary time period from 0.06 second to 0.12 second, it is seen from Figures 6(a) and 6(b), that the Fourier-based
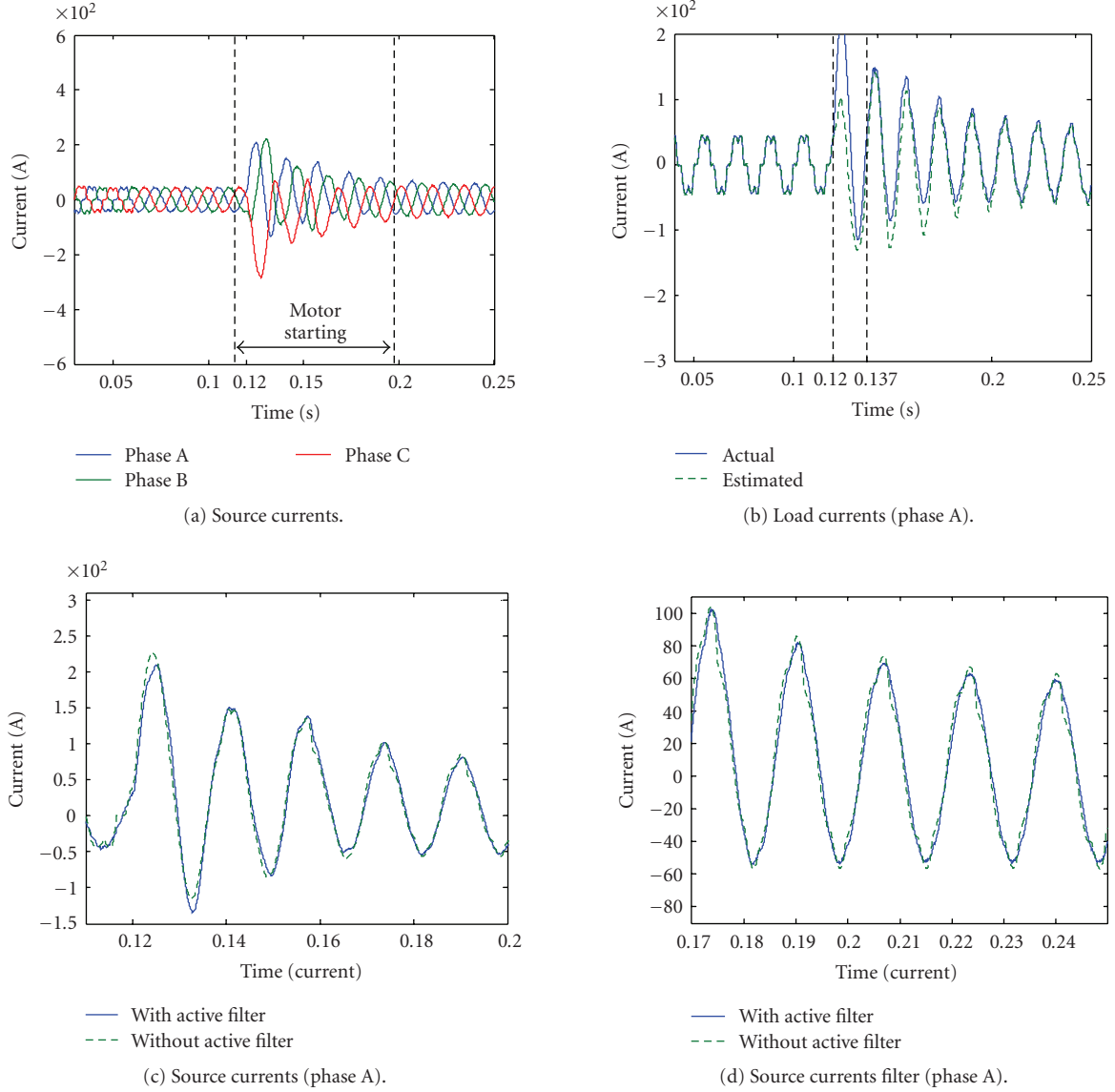
FIGURE 6: Simulation results of case 2 (FFT).

filter can filter out the stationary harmonics and the current estimated from the FFT reflects the actual current. After the motor starts at 0.12 second, one cycle, 0.0167 second, of data collection is required for the FFT function, while 0.024 second is required for the Prony analysis. After the data collections, the difference between the actual and estimated transient load currents shown in Figure 6(b) is much larger than the difference shown in Figure 5(b). Therefore, the harmonic cancellation shown in Figure 6(a) is worse than the harmonic cancellation in Figure 5(a). Additionally, the improvement of the source current shown in Figures 6(c) and 6(d) by the Fourier-based active filter is less than the improvement in Figures 5(c) and 5(d) by the Prony-based filter. Here, the results verify the deduction in Section 2.4 that the Fourier transform cannot identify exponential signals accurately. In this study, the size of the FFT analysis window is selected as one cycle of the fundamental component. Without the knowledge of the harmonic components in a signal, the results from the Fourier-based active filter could be worse with a longer analysis window.

The effectiveness of the Prony-based harmonic selective active filter to cancel transient harmonics during motor starting is verified. The Prony analysis successfully identified the damped harmonic currents, including the fundamental and the second harmonic currents, from the load currents. Using the active filter, the dominant second, fifth and seventh harmonics in the load currents are cancelled and the power quality during motor starting is improved. It is observed in Figure 5(b) that there are oscillations in the estimated load current at the beginning of motor starting. This is because the input data of parameter estimation at this time duration contains information before and after the transients begin.

5. CONCLUSIONS

In this paper, Prony analysis is applied for the power quality study when transient or time varying harmonics exhibit in power systems. The unique features of Prony analysis, such as frequency identification without prior knowledge of frequency and the ability to identify damping factors, are useful to power system quality study. The results presented in this paper verify the effectiveness of Prony analysis in the supervision and cancellation of power system transient harmonics. The Prony-based harmonic supervisor identifies transient harmonics during transformer energization more accurately than the Fourier-transform-based harmonic supervisor. With Prony analysis as the harmonic reference generation method, harmonic selective active filters cancel transient harmonics during motor starting. The Prony-based harmonic active filter cancels transient harmonics more effectively during motor starting than the Fourier-transform-based harmonic active filter does. Based on the results presented in this paper, further studies can be carried out for power quality study. Just as Prony analysis was used with harmonic selective active filters, Prony analysis may be applied to other measures to improve power quality.

The Prony-analysis-based harmonic supervisor and harmonic selective filter applied in this paper have some shortcomings. The computational speed of the nonrecursive SVD algorithm for Prony is slow. In this paper, Prony analysis is carried out offline on simulated voltage and currents. With more efficient algorithms developed, Prony analysis can be applied for online harmonic monitoring and harmonics cancellation using real-time hardware-in-loop (RT-HIL) technology. Due to the insufficient information input into Prony analysis, inaccurate harmonic estimation from Prony analysis may adversely affect controllers at the beginning of transient periods. These disadvantages of applying Prony analysis are being considered and will be improved in future studies.

APPENDIX

Table A.1: Parameters of source of test system 1.

V_{RMSLL} (kV)	f (Hz)	$R_s(\Omega)$	L_s (H)
500	60	5.55	0.221

Table A.2: Parameters of a local capacitive load of test system 1.

$R(\Omega)$	C (F)
0.6606	0.0011

Table A.3: Parameters of a three-phase transformer of test system 1.

R_1 (Ω)	L_1 (H)	$R_2(\Omega)$	L_2 (H)	R_M (Ω)	Ratio (kV/kV)
1.1111	44.4444	0.2351	9.4044	0.041	500/230

Table A.4: Transformer saturation characteristic of test system 1.

λ (p.u.)	I(p.u.)
0	0
1.20	0.0024
1.52	1.0

Table A.5: Parameters of source of test system 2.

V_{RMSLL} (V)	f (Hz)	$R_s(\Omega)$	L_s (H)
480	60	10^{-5}	10^{-6}

Table A.6: Parameters of a six-pole induction motor of test system 2.

R_s (Ω)	L_s (H)	R_r (Ω)	L_r (H)	L_M (H)	J (kgm^2)
0.294	0.00139	0.156	0.00074	0.041	0.002

Table A.7: Parameters of a rectifier load of test system 2.

R_{L} (Ω)	C_{L}(F)	$R_{\mathrm{LD}}(\Omega)$	L_{LD} (H)
15	0.004	0.001	0.003

Table A.8: Parameters of an active filter of test system 2.

V_{Ref} (V)	C_{dc} (F)	$R_{\mathrm{AF}}(\Omega)$	L_{AF} (H)
800	0.002	0.0001	0.002

Table A.9: Parameters of a PI controller of test system 2.

K_{P}	K_{I}
1.0	1.0

Table A.10: Parameters of a hysteresis controller of test system 2.

T_{on}	T_{off}	G_{on}	G_{off}
0.001	-0.001	1	0

ACKNOWLEDGMENT

REFERENCES

[1] P.-T. Cheng, S. Bhattacharya, and D. Divan, "Operations of the dominant harmonic active filter (DHAF) under realistic utility conditions," *IEEE Transactions on Industry Applications*, vol. 37, no. 4, pp. 1037–1044, 2001.

[2] P.-T. Cheng, S. Bhattacharya, and D. Divan, "Control of square-wave inverters in high-power hybrid active filter systems," *IEEE Transactions on Industry Applications*, vol. 34, no. 3, pp. 458–472, 1998.

[3] P.-T. Cheng, S. Bhattacharya, and D. Divan, "Line harmonics reduction in high-power systems using square-wave inverters-based dominant harmonic active filter," *IEEE Transactions on Power Electronics*, vol. 14, no. 2, pp. 265–272, 1999.

[4] P.-T. Cheng, S. Bhattacharya, and D. Divan, "Experimental verification of dominant harmonic active filter for high-power applications," *IEEE Transactions on Industry Applications*, vol. 36, no. 2, pp. 567–577, 2000.

[5] J. Arrillaga, B. C. Smith, N. R. Watson, and A. R. Wood, *Power System Harmonic Analysis*, John Wiley & Sons, New York, NY, USA, 1997.

[6] C. S. Moo, Y. N. Chang, and P. P. Mok, "A digital measurement scheme for time-varying transient harmonics," *IEEE Transactions on Power Delivery*, vol. 10, no. 2, pp. 588–594, 1995.

[7] S. J. Huang, C. L. Huang, and C. T. Hsieh, "Application of Gabor transform technique to supervise power system transient harmonics," *IEE Proceedings: Generation, Transmission and Distribution*, vol. 143, no. 5, pp. 461–466, 1996.

[8] J. F. Hauer, C. J. Demeure, and L. L. Scharf, "Initial results in Prony analysis of power system response signals," *IEEE Transactions on Power Systems*, vol. 5, no. 1, pp. 80–89, 1990.

[9] O. Chaari, P. Bastard, and M. Meunier, "Prony's method: an efficient tool for the analysis of earth fault currents in Petersen-coil-protected networks," *IEEE Transactions on Power Delivery*, vol. 10, no. 3, pp. 1234–1241, 1995.

[10] F. B. Hildebrand, *Introduction to Numerical Analysis*, McGraw-Hill Book, New York, NY, USA, 1956.

[11] L. Marple, "A new autoregressive spectrum analysis algorithm," *IEEE Transactions on Acoustics, Speech, and Signal Processing*, vol. 28, no. 4, pp. 441–454, 1980.

[12] P. Barone, "Some practical remarks on the extended Prony's method of spectrum analysis," *Proceedings of the IEEE*, vol. 76, no. 3, pp. 284–285, 1988.

[13] S. M. Kay and S. L. Marple Jr., "Spectrum analysis—a modern perspective," *Proceedings of the IEEE*, vol. 69, no. 11, pp. 1380–1419, 1981.

[14] E. Anderson, Z. Bai, C. Bischof, et al., *LAPACK User's Guide*, SIAM, Philadelphia, Pa, USA, 3rd edition, 1999.

[15] M. A. Johnson, I. P. Zarafonitis, and M. Calligaris, "Prony analysis and power system stability-some recent theoretical and applications research," in *Proceedings of IEEE Power Engineering Society General Meeting*, vol. 3, pp. 1918–1923, Seattle, Wash, USA, July 2000.

[16] L. Qi, L. Qian, D. Cartes, and S. Woodruff, "Initial results in Prony analysis for harmonic selective active filters," in *Proceedings of IEEE Power Engineering Society General Meeting*, p. 6, Montreal, Canada, June 2006.

[17] Hydro-Quebec, TransEnergie, SymPowerSystems For Use With Simulink, Online only, The Mathworks, July 2002.

[18] Powersim, *PSIM User's Guide Version 6.0*, Powersim, Andover, Mass, USA, June 2003.

Li Qi received her Ph.D. degree in electrical engineering from Texas A&M University in 2004. She is now an Assistant Scholar Scientist at The Center for Advanced Power Systems at Florida State University. Her research areas include power system modeling and simulations, real-time digital simulations, power system stability, and restructured electricity markets.

Lewei Qian received the B.S. and M.S. degrees in electrical engineering from Hefei University of Technology, China, in 2000 and 2003, respectively. He is currently enrolled in the doctoral program in Mechanical Engineering Department of Florida State University and is working as a Research Assistant at The Center for Advanced Power Systems at Florida State University. His research interests are active filter control, reconfigurable power conversion, and real-time digital simulations.

Stephen Woodruff received his Ph.D. degree in aerospace engineering from the University of Michigan. He is currently employed at The Center for Advanced Power Systems at Florida State University, where he works on the development of simulation and hardware-in-the-loop techniques for power systems and their application to electric ship systems.

David Cartes has been an Assistant Professor of mechanical engineering at Florida State University since January 2001. He received his Ph.D. degree in engineering science from Dartmouth College. He heads the Power Controls Lab at CAPS. His research interests include distributed control and reconfigurable systems, real-time system identification, and adaptive control. In 1994, he completed a 20-year US navy career with experience in operation, conversion, overhaul, and repair of complex marine propulsion systems.